



Deposited via The University of Leeds.

White Rose Research Online URL for this paper:

<https://eprints.whiterose.ac.uk/id/eprint/129943/>

Version: Accepted Version

Article:

Yan, S, Boyanov, MI, Mishra, B et al. (2018) U(VI) Reduction by Biogenic and Abiotic Hydroxycarbonate Green Rusts: Impacts on U(IV) Speciation and Stability Over Time. *Environmental science & technology*, 52. pp. 4601-4609. ISSN: 0013-936X

<https://doi.org/10.1021/acs.est.7b06405>

(c) 2018 American Chemical Society. This document is the Accepted Manuscript version of a Published Work that appeared in final form in *Environmental Science and Technology* after peer review and technical editing by the publisher. To access the final edited and published work see <https://doi.org/10.1021/acs.est.7b06405>

Reuse

Items deposited in White Rose Research Online are protected by copyright, with all rights reserved unless indicated otherwise. They may be downloaded and/or printed for private study, or other acts as permitted by national copyright laws. The publisher or other rights holders may allow further reproduction and re-use of the full text version. This is indicated by the licence information on the White Rose Research Online record for the item.

Takedown

If you consider content in White Rose Research Online to be in breach of UK law, please notify us by emailing eprints@whiterose.ac.uk including the URL of the record and the reason for the withdrawal request.

1 U(VI) Reduction by Biogenic and Abiotic Hydroxycarbonate Green
2 Rusts: Impacts on U(IV) Speciation and Stability Over Time
3

4 Sen Yan,^{1,2*} Maxim I. Boyanov,^{2,3} Bhoopesh Mishra,^{2,4} Kenneth M. Kemner,² and
5 Edward J. O'Loughlin^{2*}
6

7 1. School of Earth Sciences, China University of Geosciences, Wuhan, 430074, China
8 (sen.yan@cug.edu.cn)

9 2. Biosciences Division, Argonne National Laboratory, Argonne, IL, 60439, USA
10 (oloughlin@anl.gov, kemner@anl.gov)

11 3. Institute of Chemical Engineering, Bulgarian Academy of Sciences, Sofia, 1113, Bulgaria
12 (mboyanov@ice.bas.bg)

13 4. School of Chemical and Process Engineering, University of Leeds, Leeds, LS2 9JT, UK
14 (b.mishra@leeds.ac.uk)

15
The submitted manuscript has been created by UChicago Argonne, LLC, Operator of Argonne National Laboratory ("Argonne"). Argonne, a U.S. Department of Energy Office of Science laboratory, is operated under Contract No. DE-AC02-06CH11357. The U.S. Government retains for itself, and others acting on its behalf, a paid-up nonexclusive, irrevocable worldwide license in said article to reproduce, prepare derivative works, distribute copies to the public, and perform publicly and display publicly, by or on behalf of the Government. The Department of Energy will provide public access to these results of federally sponsored research in accordance with the DOE Public Access Plan. <http://energy.gov/downloads/doe-public-accessplan>

* Corresponding author (SY) phone: (86) 27-67883033; e-mail: sen.yan@cug.edu.cn; address: School of Earth Sciences, China University of Geosciences, 388 Lumo Road, Wuhan, China, 430074.

* Corresponding author (EJO) phone: (630) 252-9902; e-mail: oloughlin@anl.gov; address: Biosciences Division, Argonne National Laboratory, Building 203, Room E-137, 9700 South Cass Ave., Argonne, IL 60439-4843.

16 **ABSTRACT**

17 Green rusts (GRs) are redox active $\text{Fe}^{\text{II}}\text{-Fe}^{\text{III}}$ minerals that form in the environment via various biotic and
18 abiotic processes. Although both biogenic (BioGR) and abiotic (ChemGR) GRs have been shown to reduce
19 U^{VI} , the dynamics of the transformations and the speciation and stability of the resulting U^{IV} phases are
20 poorly understood. We used carbonate extraction and XAFS spectroscopy to investigate the products of
21 U^{VI} reduction by BioGR and ChemGR. The results show that both GRs can rapidly remove U^{VI} from
22 synthetic groundwater via reduction to U^{IV} . The initial products in the ChemGR system are solids-
23 associated U^{IV} -carbonate complexes that gradually transform to nanocrystalline uraninite over time, leading
24 to a decrease in the proportion of carbonate-extractable U from ~95% to ~10%. In contrast, solid-phase U^{IV}
25 atoms in the BioGR system remain relatively extractable, non-uraninite U^{IV} species over the same reaction
26 period. The presence of calcium and carbonate in groundwater significantly increase the extractability of
27 U^{IV} in the BioGR system. These data provide new insights into the transformations of U under anoxic
28 conditions in groundwater that contains calcium and carbonate, and have major implications for predicting
29 uranium stability within redox dynamic environments and designing approaches for the remediation of
30 uranium-contaminated groundwater.

31

32 **INTRODUCTION**

33 Uranium (U) is a contaminant at numerous uranium mining, ore processing, nuclear energy, and weapons-
34 related sites. Indeed, nearly 70% of U.S. Department of Energy facilities report groundwater contamination
35 by uranium.¹ The predominant valence states of uranium in groundwater are U^{VI} and U^{IV} ,² and the reduction
36 of soluble uranyl ($\text{U}^{\text{VI}}\text{O}_2^{2+}$) to sparingly soluble U^{IV} forms such as uraninite and non-uraninite U^{IV} species
37 has been explored as a basis for managing uranium mobility at contaminated sites. Past studies have
38 indicated that mixtures of uraninite and non-uraninite U^{IV} species can form as products of U^{VI} reduction in
39 reduced sediments.³⁻⁵ Although some of the factors controlling the formation and stability of non-uraninite
40 U^{IV} species have been determined,⁶⁻⁸ much remains unknown concerning the effects of ligands and mineral

41 surfaces on U^{IV} speciation and the stability and transformation of the U^{IV} products. Understanding the
42 structure and transformation of these U^{IV} products is crucial for understanding their long-term stability and
43 the processes controlling the fate and mobility of U in natural and engineered environments.

44

45 Green rusts (GRs) are mixed-valence Fe^{II} - Fe^{III} minerals found in redox transition zones in a variety of
46 suboxic and anoxic environments including surface waters,⁹ groundwater,^{10, 11} soils,¹²⁻¹⁴ and sediments.¹⁵⁻¹⁷

47 GRs are redox active and may play a role in the fate and transformation of many organic^{18, 19} and inorganic
48 contaminants,²⁰⁻²³ including uranium. GRs can form via various microbial and abiotic processes under
49 circumneutral to alkaline conditions in suboxic environments.²⁴⁻³¹ Biogenic (BioGR) and abiotic (ChemGR)

50 GRs have different surface properties, attributed largely to sorption of extracellular polymeric substances
51 (EPSs) on BioGRs that passivate their surface, thereby inhibiting their reactivity toward contaminants such

52 as nitrate and methyl red.^{32, 33} However, Remy et al. found no significant difference in reactivity between

53 BioGR and ChemGR with respect to the reduction of Hg^{II} .³³ In previous studies, we showed that both

54 abiotic hydroxysulfate GR³⁴ and biogenic hydroxycarbonate GR³⁵ can rapidly remove U^{VI} from solution

55 via reduction to U^{IV} in the form of uraninite nanoparticles in batch reactors containing deionized water.

56 Moreover, Latta et al. found that U^{VI} was reduced to monomeric-type U^{IV} species by three different

57 ChemGRs in deionized water containing TAPS buffer, and variable extents of U^{VI} reduction (34% to 100%)

58 were observed for hydroxycarbonate GR with and without TAPS buffer.³⁶ The chemical speciation of U^{VI}

59 can also have significant effects on its redox reactivity. For example, U^{VI} can form relatively stable and

60 soluble complexes in the presence of calcium and carbonate, which are common constituents in

61 groundwater. The formation of $Ca-UO_2-CO_3$ complexes is known to limit microbial reduction of U^{VI} to

62 U^{IV} ;³⁷ however, the effect of these complexes on the abiotic reduction of U^{VI} by Fe^{II} species is largely

63 unknown.

64

65 In this study, we examined the potential differences between BioGR and ChemGR with respect to U^{VI}

66 reduction in synthetic groundwater, particularly the speciation, transformation, and stability of the resulting

67 U^{IV} species using x-ray absorption fine structure (XAFS) spectroscopy and carbonate extraction. We
68 hypothesized that BioGR and ChemGR affect differently the speciation, transformation, and stability of
69 U^{VI} reduction products based on the presence of organic ligands and presumed differences in surface
70 properties.³²

71

72 MATERIALS AND METHODS

73 Synthesis of GRs

74 Experiments were conducted using biogenic and abiotic hydroxycarbonate GR, because hydroxycarbonate
75 GR is the most prevalent form in natural systems;^{9, 10, 38} moreover, preliminary experiments demonstrated
76 that hydroxycarbonate GR is more stable than hydroxychloride GR or hydroxysulfate GR in our synthetic
77 groundwater (data not shown), consistent with previous studies of GR stability.^{39, 40} The ChemGR was
78 synthesized using the coprecipitation method described by Etique et al.²³ Briefly, 9.341 g of ferrous sulfate
79 heptahydrate and 4.789 g of ferric sulfate hydrate were dissolved in 100 mL of deoxygenated deionized
80 water in an anoxic glovebox (N₂/H₂, 95%/5%), resulting in a ferric molar fraction ($x = [\text{Fe}^{\text{III}}]/([\text{Fe}^{\text{II}}] + [\text{Fe}^{\text{III}}])$)
81 of 0.33. Then 100 mL of a basic solution of 1008 mM NaOH and 588 mM Na₂CO₃ was added to the
82 Fe^{II}-Fe^{III} solution, corresponding to a $[\text{OH}^-]/([\text{Fe}^{\text{II}}] + [\text{Fe}^{\text{III}}])$ ratio of 2 and $[\text{CO}_3^{2-}]/([\text{Fe}^{\text{II}}] + [\text{Fe}^{\text{III}}])$ ratio of
83 7/6. A bluish-green precipitate appeared immediately. The solids were collected by centrifugation and
84 washed three times with sterile, anoxic deionized (DI) water to remove any soluble reactants.

85

86 The BioGR was obtained from the bioreduction of lepidocrocite by *Shewanella putrefaciens* CN32 as
87 described by O'Loughlin et al.³⁵ BioGR was pasteurized (65 °C for 1 h) to eliminate the potential for
88 microbial reduction of U^{VI} (a control reactor with unpasteurized BioGR was also examined). The BioGR
89 solids were collected by centrifugation and were repeatedly washed with sterile, anoxic water to promote
90 removal of cells, cell debris, and any soluble reductants. Characterization of the ChemGR and BioGR by
91 powder x-ray diffraction (pXRD) both before and after the washing procedure showed no indication of

92 changes in their crystallographic features (Figure S1). Moreover, control experiments comparing unwashed
93 BioGR and washed BioGR did not show differences in U^{VI} removal or U extraction (Figure S2), indicating
94 the washing procedure didn't affect the reactivity of the BioGR. After the final washing, GRs were re-
95 suspended in sterile deoxygenated CO_2 -free deionized water.

96

97 **Experimental Design**

98 Unless indicated otherwise, experimental setup, execution, and sample preparation were conducted under
99 anoxic conditions—typically in sealed containers in a glovebox with 3–5% H_2 in N_2 ($O_2 < 1$ ppm in the gas
100 atmosphere). The synthetic groundwater (SGW) used in our experiments was formulated to mimic the
101 composition of uranium-contaminated groundwater at the US DOE Hanford site.⁴¹ The SGW was prepared
102 by mixing three stock solutions (14.4 mM $NaHCO_3$ and 1.6 mM $KHCO_3$; 5.1 mM $MgSO_4$ and 1.2 mM
103 $CaSO_4$; and 8.8 mM $CaCl_2$) in DI-water to obtain the following composition: 1.44 mM $NaHCO_3$, 0.16 mM
104 $KHCO_3$, 0.51 mM $MgSO_4$, 0.12 mM $CaSO_4$, and 0.88 mM $CaCl_2$. No precipitates were observed in the
105 SGW and the pH was 7.9. The experimental system consisted of 50-mL polypropylene centrifuge tubes
106 with screw caps containing 40 mL of SGW, U^{VI} , and GR. SGW and U^{VI} were premixed overnight to reach
107 equilibrium before adding the GR slurry. The DI-control system contained 40 mL of anoxic DI-water, U^{VI} ,
108 and GR. Reactions were initiated by spiking with the GR slurry to provide final Fe^{II} and U^{VI} concentrations
109 of 60 mM and 1 mM, respectively. Then the slurry was mixed thoroughly with a rotator at 50 rpm. All the
110 reactions and samples were prepared in duplicate. At selected times, an aliquot of the suspension was
111 centrifuged, and the U^{VI} concentration in the supernatant was measured to determine the kinetics of U^{VI}
112 removal from solution. The extractability of U^{IV} was examined using a carbonate extraction approach via
113 the addition of 0.1 mL of suspension to 0.9 mL of anoxic 2 M Na_2CO_3 . After 24 h, the mixture was
114 centrifuged, and the supernatant was retained for measurement of extracted U. Our preliminary assessment
115 of carbonate extraction efficiency indicated that 1.8 M carbonate was sufficient to extract the labile U
116 associated with GR solids under our experimental conditions and the extraction efficiency did not change
117 after 24 h of extraction (Figure S3). The solid samples used for XAFS analysis were collected by filtration
es-2017-06405v

118 on 0.22- μm nylon filters, and then the filter membrane with the hydrated solids was sealed with 8.4- μm -
119 thick Kapton film and tape under anoxic conditions.

120

121 **Analytical procedures**

122 The pXRD analysis was performed with a Rigaku MiniFlex x-ray diffractometer with Ni-filtered Cu $K\alpha$
123 radiation. Samples for pXRD analysis were collected by filtration on 25-mm, 0.22- μm nylon filters and
124 covered with 8.4- μm -thick Kapton film under anoxic conditions. The samples were scanned between 5°
125 and $80^\circ 2\theta$ at a speed of $2.5^\circ 2\theta \text{ min}^{-1}$. The pXRD patterns were analyzed with the JADE 6 software package
126 (MDI, Livermore, California). The Fe(II) concentrations in the reactors and GR stock suspensions were
127 determined using the ferrozine method⁴² after digestion with anoxic 2 M HCl in the anoxic glovebox.
128 Samples for measurement of aqueous U in GR suspensions were prepared via centrifugation at 13,000 g
129 for 2 min inside an anoxic glovebox with 3–5% H_2 in N_2 ($\text{O}_2 < 1$ ppm in the gas atmosphere). Preliminary
130 experiments didn't show any difference in aqueous U concentrations between samples centrifuged then
131 filtered through 0.22 μm membrane filters and samples only centrifuged, therefore subsequent samples
132 were only centrifuged. The aqueous and extracted U^{VI} concentrations in the reactors were measured using
133 a Chemchek kinetic phosphorescence analyzer (KPA-11) following the procedure developed by Sowder et
134 al. and Dong et al.^{43,44} Selected samples were also analyzed by inductively coupled plasma-optical emission
135 spectroscopy (ICP-OES). The data obtained by these two methods were consistent, with a difference always
136 less than 6%. The speciation of U in the solid phases of the reactors was analyzed by x-ray absorption
137 spectroscopy at sectors 10-ID and 10-BM of the Advanced Photon Source, using a setup described in more
138 detail in the Supporting Information (SI).³⁴⁻³⁶ Briefly, x-ray absorption near-edge spectroscopy (XANES)
139 and extended x-ray absorption fine structure (EXAFS) scans at the U L_{III} edge (17,166 eV) were collected
140 in quick scanning mode (3 min each). The final spectrum was produced by averaging 30–50 quick EXAFS
141 scans. The data were processed using ATHENA, and the contributions of distinct U^{IV} species in the EXAFS
142 spectra were quantified using linear combination (LC) fitting.⁴⁵ Previously measured spectra from a

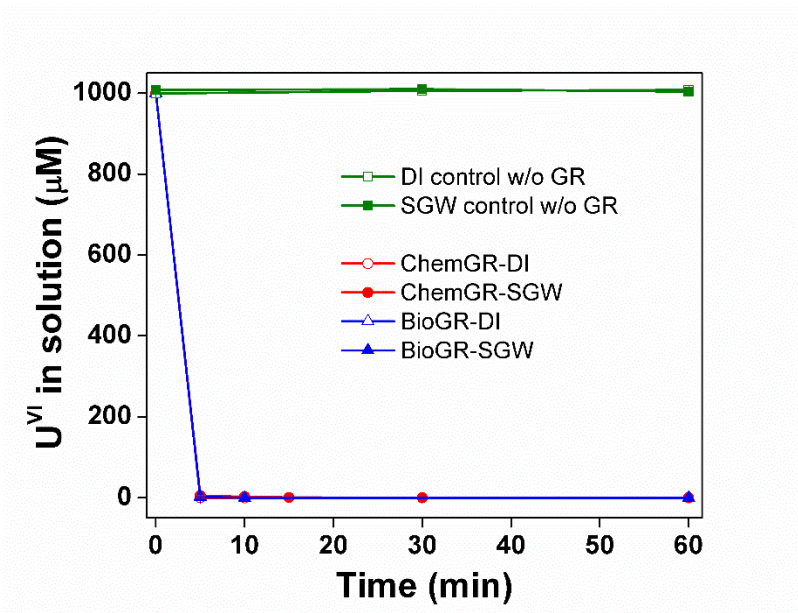
143 nanoparticulate uraninite standard and U^{IV} -carbonate complexes were used as end members.⁶ Additional
144 details of the XAFS data collection and analysis are provided in the SI.

145

146 **RESULTS AND DISCUSSION**

147 **U^{VI} removal by GR**

148 U^{VI} was rapidly removed from solution in both the ChemGR and BioGR systems (Figure 1). Since the total
149 U concentration in the systems were supersaturated with respect to schoepite, it is possible that the loss of
150 U^{VI} from solution could be due in part to precipitation of a U^{VI} phase such as schoepite. However the
151 aqueous U^{VI} concentrations remained stable at $\sim 1000 \mu M$ in the control systems without GR (Figure 1)
152 and there was no visual indication of precipitate formation over the period of observation; thus the rapid
153 initial removal of U^{VI} can be attributed to uptake by GR. In the DI-water control system, over 99% of U^{VI}
154 was removed within 5 min by ChemGR and BioGR, which is comparable to the results reported by
155 O'Loughlin et al.³⁵ In the SGW system, U^{VI} was also rapidly removed from solutions by ChemGR and
156 BioGR, indicating both GRs are likely to be effective for removal of U^{VI} from groundwater even in the
157 presence of calcium and carbonate. There was no significant difference in the kinetics of U^{VI} removal from
158 solution between ChemGR and BioGR. This is similar to the result in Remy et al., which showed no
159 significant difference between ChemGR and BioGR with respect to Hg^{II} reduction.³³



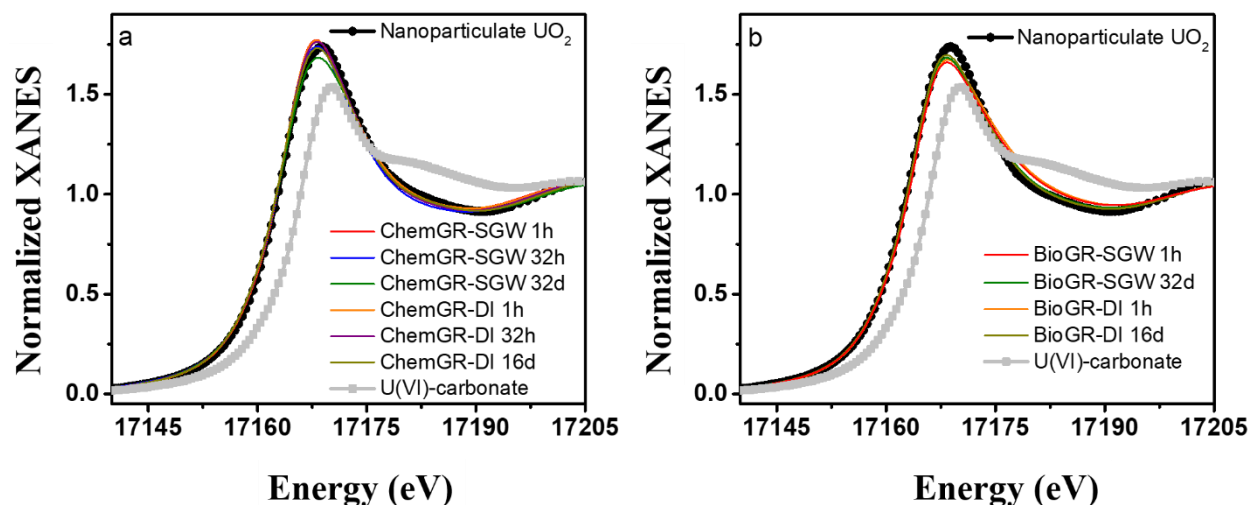
160
 161 **Figure 1.** Removal of U^{VI} from solution by ChemGR and BioGR in deionized water (DI) and synthetic
 162 groundwater (SGW) systems.

163
 164 **U^{VI} Is Reduced to U^{IV} by GR**

165 U L_{III} edge XANES spectra (Figure 2) show that under all experimental conditions the U associated with
 166 the solids is predominantly U^{IV} . The edge energy position and the spectral shape of all XANES spectra are
 167 similar to the U^{IV} standard, indicating that over 95% of the U in the solid phase is U^{IV} . Small amounts of
 168 U^{VI} were observed only in the 1 h BioGR samples from the DI-water and SGW systems (small shoulder
 169 near 17,180 eV in Figure 2), which were quantified as ~17% of solid-phase U based on LC fits of the
 170 XANES data with U^{IV} and U^{VI} standards (analysis not shown). Together with the similar and rapid uptake
 171 kinetics in all systems (Figure 1), the XANES results suggest that an adsorption step occurring on the
 172 timescale of minutes is followed by a fast (<1 h) reduction of U^{VI} to U^{IV} . Similar uptake profiles (i.e., rapid
 173 uptake followed by reduction) have been observed in previous studies with GR, as well as with other Fe^{II}
 174 phases.^{35, 36, 46-48}

175

176

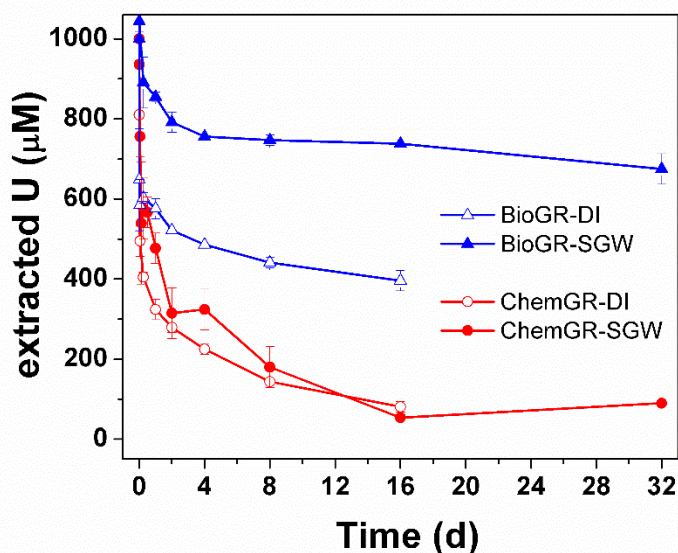


177
 178 **Figure 2.** U L_{III} edge XANES spectra for (a) ChemGR and (b) BioGR at various times in deionized water
 179 (DI) or synthetic groundwater (SGW) systems compared with U^{IV} and U^{VI} standards.

180
 181 **Extraction of U by Carbonate in the ChemGR and BioGR Systems**
 182 Carbonate has been shown to extract U associated with mineral and biological solids, in both the U^{VI} ⁴⁹⁻⁵¹
 183 and the U^{IV} valence states.^{5, 51} The latter studies also showed that U^{IV} is less extractable when present as
 184 uraninite relative to the more labile monomeric species (e.g., adsorbed or ligand-complexed U^{IV}). The
 185 XANES results indicate that U^{VI} was reduced to U^{IV} in both the ChemGR and BioGR reactors and we used
 186 a 1.8 M carbonate extraction method to evaluate the relative stability of U^{IV} in these two systems. As shown
 187 in Figure 3, the pool of labile (i.e., carbonate-extractable) U is significantly larger in the BioGR system
 188 than in the ChemGR system. The pools of extractable U in both systems gradually decreased over time until
 189 they reached steady state, suggesting that the U^{IV} species aged to a more stable form over a period of days.
 190 For instance, in SGW, about 85% of the U in the solids could be extracted in the BioGR system after 24 h,
 191 but after 4 d of reaction the carbonate-extractable U decreased to 70% and remained unchanged over the
 192 following 28 d. Similarly, in the ChemGR system about 50% of U in the solids could be extracted after
 193 24 h, only 30% after 4 d, and only 10% after the system reached steady state at 16 d. In the reactors with
 194 BioGR, more U was extractable in SGW than in the DI-water control, which suggests that the presence of

195 calcium and carbonate during U^{VI} reduction by BioGR increased the extractability of U in the system. In
 196 contrast, the ChemGR systems showed no significant difference in U extractability between the DI-water
 197 and SGW solution conditions.

198



199

200 **Figure 3.** Changes in carbonate-extractable U over time in ChemGR and BioGR systems with deionized
 201 water (DI) or synthetic groundwater (SGW). The error bars denote the standard error of measurements
 202 made on duplicate bottles.

203

204 When interpreting the lability of solid-phase U^{IV} to carbonate extraction we need to consider the valence
 205 state of U released in solution. Stoliker et al.⁵ concluded that anoxic carbonate extractions of U^{IV} resulted
 206 in dissolved U^{VI} and suggested that the change in thermodynamic conditions promoted back-transfer of
 207 electrons from U^{IV} to Fe^{III} in the same sediment matrix that originally reduced U^{VI} . It is possible that U^{IV}
 208 reoxidized to U^{VI} here as well, since the 1.8 M Na_2CO_3 added during extraction significantly increased the
 209 pH values in the SGW ChemGR and BioGR systems from 8.4 to 11.9 and from 8.0 to 11.8, respectively,
 210 and the Eh increased from -674 mV to -471 mV, and from -706 mV to -507 mV, respectively. Figure S4
 211 presents the XANES data from the carbonate extraction supernatants, showing that predominantly U^{VI} was

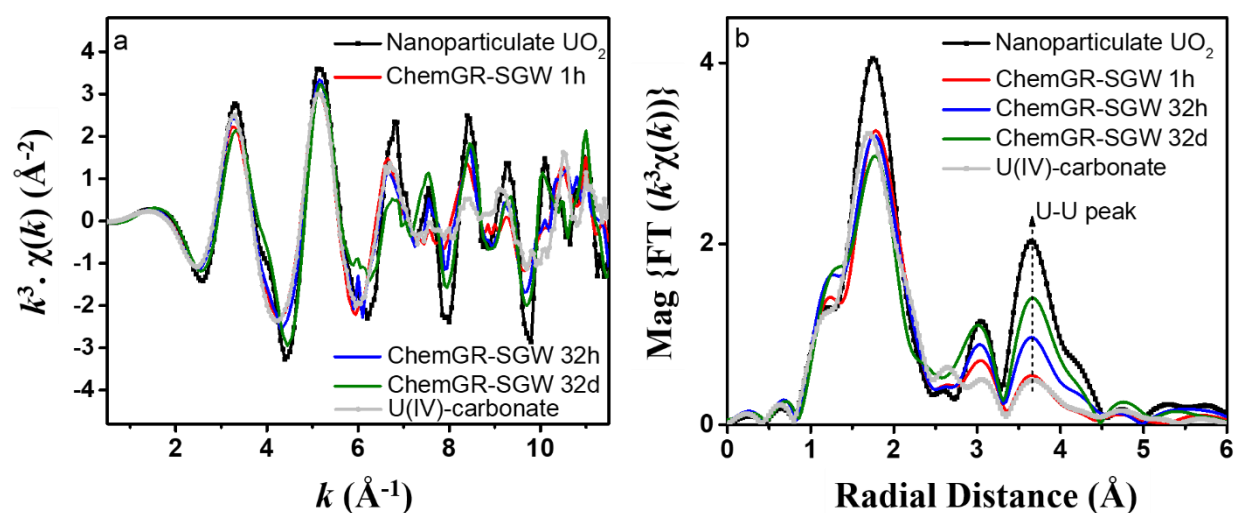
212 released in solution. We observed the same U concentrations by kinetic phosphorescence analysis before
213 and after oxidation of the extraction supernatants in air (data not shown), also showing that predominantly
214 U^{VI} was present in the extracts. Both of the above suggest that the change in solution conditions caused by
215 the addition of carbonate resulted in the reoxidation of solids-associated U^{IV} leading to the release of U^{VI} .
216 However, the possibility that U^{IV} was first removed from the solids as U^{IV} -carbonate complexes and then
217 reoxidized as a soluble species by contact with Fe^{III} cannot be excluded by the current data. Thus, the data
218 in Figure 3 may indicate either susceptibility of the reduced U^{IV} phases to oxidation under the conditions
219 of the extractions or susceptibility of U^{IV} to complexation by carbonate, if the latter is the rate determining
220 step in the observed oxidative release. Regardless of the actual oxidation mechanism during extraction, the
221 different extractability of U^{IV} in the ChemGR and BioGR systems suggest differences in the initial U^{IV}
222 speciation of U^{IV} produced in these two systems, as confirmed by the EXAFS results below.

223

224 **U Speciation in the ChemGR and BioGR Systems**

225 The observed differences in U^{IV} extractability suggest differences in U^{IV} speciation between the ChemGR
226 and BioGR systems. We used EXAFS spectroscopy to examine the molecular structure around the U^{IV}
227 atoms in both systems. In the ChemGR system, the EXAFS spectra show systematic trends as a function of
228 reaction time, in both the SGW (Figure 4) and the DI-water control (Figure S5) systems. Specifically, the
229 Fourier transform (FT) of the EXAFS data for the 1-h reaction time samples lacks significant amplitude
230 around $R + \Delta = 3.7 \text{ \AA}$, where the U coordination shell contributes in the uraninite standard. The
231 experimental spectra from the 1 h samples closely resemble that of a previously characterized U^{IV} -carbonate
232 complex produced by bacteria,⁶ both in the phase and amplitude of the $\chi(k)$ data, as well as in the features
233 of the FT (Figures 4 and S5). The spectral resemblance suggests that U^{IV} in the ChemGR system has the
234 same local structure as this previously characterized U^{IV} -carbonate complex,⁶ but is possibly associated
235 here with the minerals in our system as a ternary or an outer-sphere surface complex. There is a consistent
236 increase in the amplitude of the U peak with reaction time, and the samples at 16 d and 32 d approach the
237 nanoparticulate uraninite standard. The real part of the FT EXAFS also approaches the uraninite standard

238 over the duration of the reaction, showing an increase in the U signal and a slight decrease in the bond
 239 distance of O in the first shell (Figures S6 and S7). These spectral trends suggest that initially the entire
 240 budget of U associated with the solid phase of ChemGR is predominantly in a U^{IV} -carbonate complex,
 241 which then gradually transforms to a predominant nanoparticulate uraninite phase over the 32-d reaction
 242 period.
 243



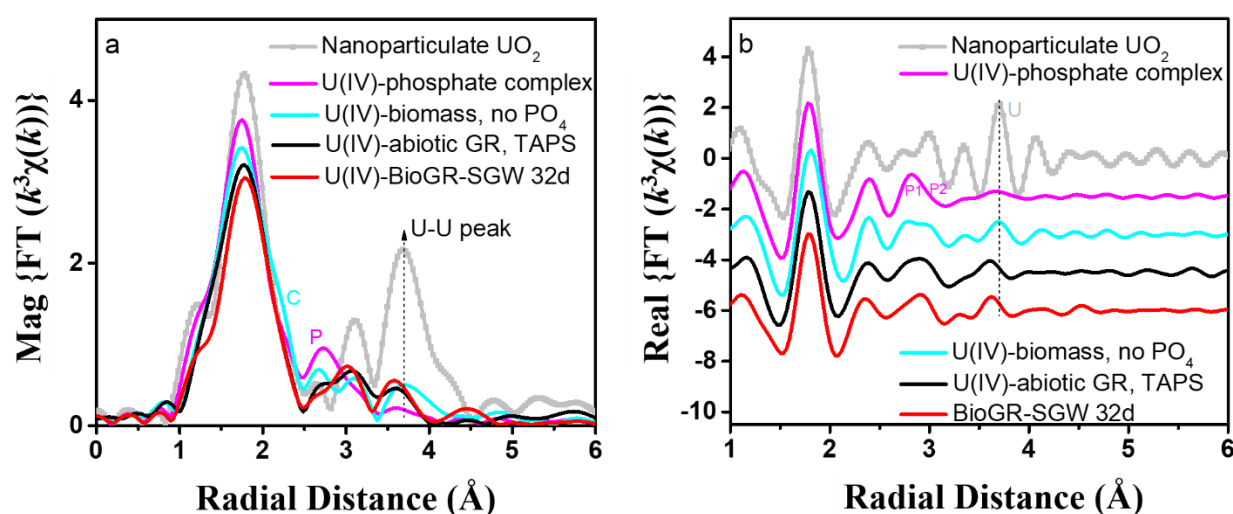
244
 245 **Figure 4.** U L_{III} edge (a) k^3 -weighted EXAFS data and (b) Fourier transformed (FT) EXAFS spectra for
 246 ChemGR in the synthetic groundwater (SGW) system after 1 h, 32 h, and 32 d, compared with
 247 nanoparticulate uraninite and U^{IV} -carbonate standards. The vertical dashed line indicates the peak in the FT
 248 EXAFS resulting from the contribution of the U shell in uraninite. The FT is within the data range $k = 2.2$ –
 249 10.4\AA^{-1} using $1.0\text{-}\text{\AA}^{-1}$ -wide Hanning windowsills. Significant spectral similarity is evident between the 1 h
 250 sample (red line) and a previously characterized U^{IV} -carbonate complex⁶ (grey symbols).

251
 252
 253 The proportions of solid-phase U species suggested by the qualitative analysis were quantified by LC fitting
 254 of the EXAFS spectra. We used previously characterized spectra of nanoparticulate uraninite and a U^{IV} -
 255 carbonate complex as end members.⁶ The data from the ChemGR systems after 1 h, 32 h and 32 d indicate

256 an increasing contribution of the uraninite phase from 8% to 25% to 77% in SGW and from 24% to 33%
257 to 75% in DI-water (Table S1) and a general trend of a higher proportion of uraninite in the DI-water system
258 compared to the SGW system. However, the difference between the two solution conditions is within the
259 uncertainty associated with the LC analysis (~10%), so uraninite formation in the SGW system is inhibited
260 only within the first hour of reaction time. Similar proportions of adsorbed U^{IV} species and nanoparticulate
261 uraninite were observed in the previous study by Latta et al.,³⁶ in which chemogenic carbonate-GR was
262 reacted with U^{VI} in DI water for 3–4 days (58% uraninite, LC analysis shown in Figure S8). Taken together,
263 the carbonate extraction data (Figure 3) and the LC analysis support a reaction sequence whereby an initial
264 labile U^{IV}-carbonate species is formed following the electron transfer between ChemGR and adsorbed U^{VI},
265 which then transforms over time to a more stable (i.e., less extractable) nanoparticulate uraninite form.

266
267 The behavior of U^{IV} in the BioGR system is significantly different compared to its behavior in the ChemGR
268 system. The U EXAFS data in the BioGR system are the same for the 16-d and 32-d samples in DI water
269 and SGW (Figure S9), which indicates lack of evolution of the U^{IV} species over the reaction period and
270 lack of dependence of the U^{IV} product on solution conditions. The 32-d BioGR-SGW spectra were highly
271 reproducible for the pasteurized sample and the unpasteurized control, which suggests that biological
272 processes did not play a role in the final U^{IV} speciation. The spectrum with the best signal-to-noise ratio
273 (BioGR-SGW, 32 d) was used for comparison to U^{IV} standards and for structural analysis. The spectra of
274 the standards were collected previously at the same beamline and include nanoparticulate uraninite,⁶
275 aqueous U^{IV} obtained by dissolving UO₂ in 0.5 M sulfuric acid,⁵² monomeric U^{IV} complexed to magnetite,⁵²
276 U^{IV} complexed to phosphate, and U^{IV} complexed to biomass without phosphate.^{6,53} Data comparisons (not
277 shown) between the BioGR sample and the aqueous U^{IV} standard or U^{IV} complexed to magnetite indicated
278 significant differences, allowing exclusion of an outer-sphere surface complexation mechanism or the
279 inner-sphere complexation mechanism with increased U^{IV}-O coordination (9–10 O atoms) such as that
280 observed previously for magnetite.⁵² The position and amplitude of the main O peak in the FT EXAFS of
281 the BioGR sample (Figure 5) is similar to that in the standards with 8-coordinated U^{IV}. The lack of a U-U
es-2017-06405v

282 backscattering signal near $R + \Delta = 3.8 \text{ \AA}$ in the BioGR data (Figure 5) excludes nanoparticulate uraninite
 283 as the predominant U^{IV} phase (in other words, <10% of total U may be present as uraninite). When
 284 compared to the spectra of U^{IV} associated with biomass in the presence and absence of phosphate,⁶ the
 285 BioGR spectrum lacks the features assigned previously to complexation of U^{IV} by a phosphate or a R-COO
 286 group (indicated by P and C in Figure 5). The BioGR spectrum is nearly identical to that of U^{IV} produced
 287 in a previous study by reacting U^{VI} in TAPS buffer with chemically synthesized GR.³⁶
 288



289 **Figure 5.** Comparison of the EXAFS data from the BioGR system to U^{IV} standards. (a) Magnitude of the
 290 Fourier transformed k^3 -weighted EXAFS data; (b) real part of the Fourier transformed k^3 -weighted EXAFS
 291 data. The shoulder in the first shell of the FT magnitude spectrum of the U^{IV} -biomass standard, representing
 292 the contribution of C, and the peak where P atoms contribute in the spectrum of the U^{IV} -phosphate standard
 293 are indicated, as determined from previous analyses.⁶ The vertical dashed line indicates the signal from the
 294 U backscattering atom in uraninite. P1 and P2 indicate the approximate positions of the signals from the bi-
 295 and mono-dentate bound phosphate groups. The spectrum of U^{IV} in the abiotic GR TAPS buffer system is
 296 taken from Latta et al.³⁶ The Fourier transform is within the data range $k = 2.2\text{--}10.4 \text{ \AA}^{-1}$ using $1.0\text{-}\text{\AA}^{-1}$ -wide
 297 Hanning windowsills.
 298
 299

300 In light of the similarity between the U+BioGR data and the data from U+chemical GR in the TAPS buffer
301 from Latta et al.,³⁶ the EXAFS model from that work was applied to fit the U+BioGR data. The model
302 included a near-neighbor O shell, an Fe shell, and an outer O shell, and produced the best simultaneous fit
303 of the data at k-weights of k^1 , k^2 , and k^3 in the Fourier transform (Figure S10 and Table S2). The refined
304 parameters show that the average U-O distance in the BioGR system is $2.35 \pm 0.01 \text{ \AA}$, which is similar to
305 the U-O distance in 8-coordinated U^{IV} species such as nanoparticulate uraninite ($2.32 \pm 0.01 \text{ \AA}$) and
306 phosphate-complexed U^{IV} ($2.33 \pm 0.01 \text{ \AA}$), but significantly shorter than that of 9–10 coordinated U^{IV}
307 species such as aqueous U^{IV} or U^{IV} adsorbed to the $=FeO$ sites in magnetite ($2.42 \pm 0.02 \text{ \AA}$).⁵² The lower
308 amplitude of the O-shell peak in the BioGR data relative to nanoparticulate uraninite or phosphate-
309 complexed U^{IV} results from a slight decrease in average coordination number and a slight increase in the
310 disorder (Debye-Waller factor) relative to the standards. Attempts to model the BioGR data with the second
311 shell U paths used to fit the nanoparticulate uraninite data indicated that the signal between $R + \Delta = 3.0$ –
312 4.0 \AA is inconsistent with U. Similarly, EXAFS modeling efforts based on the ningyoite $CaU^{IV}(PO_4)_2$
313 structure representing U^{IV} -phosphate complexation were also unsuccessful.^{6, 54}

314
315 The refined structural model with an O, Fe, and O coordination shells is consistent with adsorption of U^{IV}
316 to the brucite layer in the GR structure or possibly to other Fe transformation products in the system, rather
317 than complexation to the carbonate anions in the interlayer or to residual biological components in the
318 BioGR system. Association of U^{IV} with Fe redox products has been observed before in laboratory and
319 natural systems.^{3, 55} The nearly identical U EXAFS data in the BioGR system here and in chemical GR
320 systems studied previously³⁶ (Figure 5) also suggest U^{IV} association with the iron oxides rather than with a
321 biological component. However, it should be noted that the adsorbed U^{IV} species in the carbonate GR
322 reactors of Latta et al.³⁶ were observed only in the presence of TAPS buffer, whereas significant
323 nanoparticulate uraninite formation occurred in DI water (LC fit shown in Figure S8). Thus, although
324 carbonate GRs adsorb U^{IV} atoms at the $\equiv FeO$ sites, the stability of adsorbed U^{IV} with respect to desorption

325 and uraninite formation appears dependent on the presence of residual organic components or buffers.
326 Recent studies have also identified U^{IV} -organic matter complexation in field samples.⁵⁶ This indirect effect
327 of organic molecules on the stability of reduced U is important in an environmental context and needs to
328 be elucidated in further studies with controlled addition of organic matter. Stabilization of non-uraninite
329 U^{IV} in biogenic GR reactors was also observed in the previous study by O'Loughlin et al.³⁵ Although the
330 EXAFS data were interpreted at the time as a highly disordered uraninite phase, a comparison between the
331 BioGR data here and in the previous study³⁵ reveals that the data are the same within measurement
332 uncertainty (Figure S11). Thus, the analysis and conclusions presented above can be directly applied to the
333 data in O'Loughlin et al.³⁵ An EXAFS model with O, Fe, and O shells that is conceptually similar to the
334 U^{IV} adsorption mechanism determined in our study was also fit to the data from monomeric U^{IV} in magnetite
335 solids at low U:magnetite ratios.⁵² However, the U-O and U-Fe distances refined for the BioGR samples
336 are significantly shorter than in the U^{IV} -magnetite complexes (2.35 Å vs. 2.42 Å, and 3.49 Å vs. 3.59 Å,
337 respectively). This indicates a different binding mechanism of U^{IV} to BioGR relative to that in magnetite
338 and suggests that the arrangement of the $\equiv FeO$ sites plays a significant role in the complexation of U^{IV} to
339 iron oxide surfaces.

340
341 Based on the speciation for the BioGR and ChemGR systems, the persistence of adsorbed U^{IV} species in
342 the BioGR system over the 32-d reaction period can explain their consistently high extractability with
343 carbonate (Figure 3), whereas the transformation of adsorbed U^{IV} to uraninite in the ChemGR system can
344 explain the significant decrease in U^{IV} extractability over time. Figure 3 also reveals a relatively higher
345 extractability of U^{IV} in SGW compared to the DI-water samples within the BioGR system. However, the
346 EXAFS data show no significant differences in the U spectra between the BioGR reactors (Figure S9). This
347 suggests that the molecular structure of U alone cannot explain the observed differences in U extractability.
348 It is possible that components of the SGW solution affect U speciation in the BioGR system in a way that
349 is not apparent in the EXAFS spectra (e.g., outer-sphere complexation) or that the different solution
350 compositions affect particle size or aggregation and thus the ability of carbonate to reach and extract the

351 U^{IV} complexes. It is also possible that interaction between the biological components and DI water versus
352 SGW affects the efficiency of the carbonate extraction of the same U^{IV} species.

353

354 **Environmental implications**

355 The reduction of soluble uranyl to less soluble U^{IV} species is a key process in the biogeochemistry of U in
356 both natural and engineered environments under suboxic to anoxic conditions. However, U is not typically
357 present at high enough concentrations to control the redox state of a given environment, therefore the
358 reduction of U^{VI} is often coupled to that of a more abundant redox active element such as Fe. As previously
359 mentioned, GRs have been identified in Fe^{III}/Fe^{II} transitions zones in a variety of natural environments^{9, 11-}
360 ¹⁷ and engineered systems such as Fe^0 permeable reactive barriers^{57, 58} where due to their effectiveness as
361 reductants for U^{VI} , they may play a role in U speciation thereby impacting U fate and transport in these
362 environments. Our results showing differences in the speciation of the U^{IV} products resulting from the
363 reduction of U^{VI} by biogenic GR compared to chemogenic GR as well as previous studies demonstrating
364 differential reactivity between biogenic and chemogenic Fe^{II} phases,^{32, 33, 47 59} highlight the importance of
365 identifying the processes leading to the in situ formation of these reactive species in understanding their
366 potential role in contaminant fate and transport. However, contaminant speciation also plays a critical role.
367 Calcium and carbonate are ubiquitous components in U-contaminated groundwater. According to
368 equilibrium thermodynamic calculations, U^{VI} can form stable ternary calcium-uranyl-carbonate complexes
369 in groundwater that contains calcium and carbonate.⁴⁴ Theoretically, the stable ternary complex of U^{VI} is a
370 less thermodynamically favorable electron acceptor than the uranyl hydroxyl complex, which leads to a
371 decrease in the rate and extent of U^{VI} reduction.^{44, 50} Previous studies demonstrated that the presence of
372 calcium and carbonate at millimolar concentrations can cause a significant decrease in the rate and extent
373 of bacterial U^{VI} reduction.^{37,60} However, our results show that the potential for formation of ternary calcium-
374 uranyl-carbonate complexes did not have an observable effect on the rate or extent of reduction of U^{VI} by
375 ChemGR and BioGR in synthetic groundwater containing calcium and carbonate. Thus, GRs (whether

376 synthetic or the product of microbial Fe redox transformations) could provide a more effective means of
377 reducing the concentration of uranium in contaminated groundwater than anaerobic U^{VI}-reducing bacteria.

378

379 **ACKNOWLEDGEMENTS**

380 The authors thank Carolyn Steele and the anonymous reviewers for their thoughtful reviews of the
381 manuscript. This research was supported by the National Natural Science Foundation of China (41303084
382 and 41521001); the 111 Program (State Administration of Foreign Experts Affairs & the Ministry of
383 Education of China, grant B18049); the Fundamental Research Funds for the Central Universities, China
384 University of Geosciences-Wuhan (CUG170402 and CUG170104); and the Subsurface Science Scientific
385 Focus Area (SFA) at Argonne National Laboratory funded by the Subsurface Biogeochemical Research
386 Program, Office of Biological and Environmental Research, Office of Science, U.S. Department of Energy
387 (DOE), under contract DE-AC02-06CH11357. Use of the Advanced Photon Source was supported by the
388 U.S. Department of Energy, Office of Science, Office of Basic Energy Sciences. We thank the
389 MRCAT/EnviroCAT beamline staff at the Advanced Photon Source for assistance during XAFS data
390 collection. MRCAT/EnviroCAT operations are supported by DOE and the MRCAT/EnviroCAT member
391 institutions.

392

393 **SUPPORTING INFORMATION AVAILABLE**

394 The Supporting Information includes pXRD patterns of ChemGR and BioGR, a comparison of the
395 reactivity of washed and unwashed BioGR, assessments of carbonate extraction efficiency, details of
396 XAFS data collection and analysis, and supplemental XAFS spectra. This material is available free of
397 charge via the Internet at <http://pubs.acs.org>.

398

399 REFERENCES

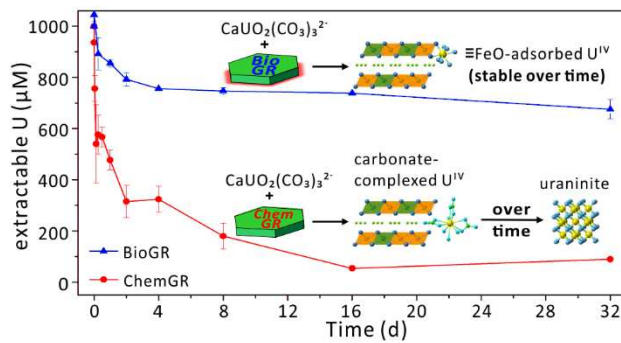
- 400 (1) Riley, R. G.; Zachara, J. M. *Chemical contaminants on DOE lands and selection of*
401 *contaminant mixtures for subsurface science research*; U.S. Department of Energy: Washington,
402 DC, 1992.
- 403 (2) O'Loughlin, E. J.; Boyanov, M. I.; Antonopoulos, D. A.; Kemner, K. M., Redox processes
404 affecting the speciation of technetium, uranium, neptunium, and plutonium in aquatic and
405 terrestrial environments. In *Aquatic Redox Chemistry*, Tratnyek, P. G., Grundl, T.J., Haderlein,
406 S.B., Ed. 2011; pp 477-517.
- 407 (3) Kelly, S. D.; Kemner, K. M.; Carley, J.; Criddle, C.; Jardine, P. M.; Marsh, T. L.; Phillips,
408 D.; Watson, D.; Wu, W. M. Speciation of uranium in sediments before and after in situ
409 biostimulation. *Environ. Sci. Technol.* **2008**, *42* (5), 1558-1564.
- 410 (4) Bargar, J. R.; Williams, K. H.; Campbell, K. M.; Long, P. E.; Stubbs, J. E.; Suvorova, E. I.;
411 Lezama-Pacheco, J. S.; Alessi, D. S.; Stylo, M.; Webb, S. M.; Davis, J. A.; Giammar, D. E.;
412 Blue, L. Y.; Bernier-Latmani, R. Uranium redox transition pathways in acetate-amended
413 sediments. *Proc. Natl. Acad. Sci. U. S. A.* **2013**, *110* (12), 4506-4511.
- 414 (5) Stoliker, D. L.; Campbell, K. M.; Fox, P. M.; Singer, D. M.; Kaviani, N.; Carey, M.; Peck, N.
415 E.; Bargar, J. R.; Kent, D. B.; Davis, J. A. Evaluating chemical extraction techniques for the
416 determination of uranium oxidation state in reduced aquifer sediments. *Environ. Sci. Technol.*
417 **2013**, *47* (16), 9225-9232.
- 418 (6) Boyanov, M. I.; Fletcher, K. E.; Kwon, M. J.; Rui, X.; O'Loughlin, E. J.; Loffler, F. E.;
419 Kemner, K. M. Solution and microbial controls on the formation of reduced U(IV) species.
420 *Environ. Sci. Technol.* **2011**, *45* (19), 8336-8344.
- 421 (7) Latta, D. E.; Kemner, K. M.; Mishra, B.; Boyanov, M. I. Effects of calcium and phosphate on
422 uranium(IV) oxidation: Comparison between nanoparticulate uraninite and amorphous U^{IV}-
423 phosphate. *Geochim. Cosmochim. Acta* **2016**, *174*, 122-142.
- 424 (8) Boyanov, M. I.; Latta, D. E.; Scherer, M. M.; O'Loughlin, E. J.; Kemner, K. M. Surface area
425 effects on the reduction of U^{VI} in the presence of synthetic montmorillonite. *Chem. Geol.* **2017**,
426 *464*, 110-117.
- 427 (9) Zegeye, A.; Bonneville, S.; Benning, L. G.; Sturm, A.; Fowle, D. A.; Jones, C.; Canfield, D.
428 E.; Ruby, C.; MacLean, L. C.; Nomosatryo, S.; Crowe, S. A.; Poulton, S. W. Green rust
429 formation controls nutrient availability in a ferruginous water column. *Geology* **2012**, *40* (7),
430 599-602.
- 431 (10) Christiansen, B. C.; Balic-Zunic, T.; Dideriksen, K.; Stipp, S. L. S. Identification of green
432 rust in groundwater. *Environ. Sci. Technol.* **2009**, *43* (10), 3436-3441.
- 433 (11) Johnson, C. A.; Freyer, G.; Fabisch, M.; Caraballo, M. A.; Kusel, K.; Hochella, M. F.
434 Observations and assessment of iron oxide and green rust nanoparticles in metal-polluted mine
435 drainage within a steep redox gradient. *Environ. Chem.* **2014**, *11* (4), 377-391.
- 436 (12) Trolard, F.; Génin, J. M. R.; Abdelmoula, M.; Bourrié, G.; Humbert, B.; Herbillon, A.
437 Identification of a green rust mineral in a reductomorphic soil by Mössbauer and Raman
438 spectroscopies. *Geochim. Cosmochim. Acta* **1997**, *61* (5), 1107-1111.
- 439 (13) Génin, J. M. R.; Bourrié, G.; Trolard, F.; Abdelmoula, M.; Jaffrezic, A.; Refait, P.; Maitre,
440 V.; Humbert, B.; Herbillon, A. Thermodynamic equilibria in aqueous suspensions of synthetic
441 and natural Fe(II)-Fe(III) green rusts: Occurrences of the mineral in hydromorphic soils.
442 *Environ. Sci. Technol.* **1998**, *32* (8), 1058-1068.

- 443 (14) Feder, F.; Trolard, F.; Klingelhofer, G.; Bourrie, G. In situ Mossbauer spectroscopy:
444 Evidence for green rust (fougerite) in a gleysol and its mineralogical transformations with time
445 and depth. *Geochim. Cosmochim. Acta* **2005**, *69* (18), 4463-4483.
- 446 (15) Bender Koch, C.; Morup, S. Identification of Green Rust in an Ochre Sludge. *Clay Minerals*
447 **1991**, *26* (4), 577-582.
- 448 (16) Bearcock, J. M.; Perkins, W. T.; Dinelli, E.; Wade, S. C. Fe(II)/Fe(III) 'green rust'
449 developed within ochreous coal mine drainage sediment in South Wales, UK. *Mineralogical*
450 *Magazine* **2006**, *70* (6), 731-741.
- 451 (17) Root, R. A.; Dixit, S.; Campbell, K. M.; Jew, A. D.; Hering, J. G.; O'Day, P. A. Arsenic
452 sequestration by sorption processes in high-iron sediments. *Geochim. Cosmochim. Acta* **2007**, *71*
453 (23), 5782-5803.
- 454 (18) Larese-Casanova, P.; Scherer, M. M. Abiotic transformation of hexahydro-1,3,5-trinitro-
455 1,3,5-triazine (RDX) by green rusts. *Environ. Sci. Technol.* **2008**, *42* (11), 3975-3981.
- 456 (19) O'Loughlin, E. J.; Burris, D. R. Reduction of halogenated ethanes by green rust. *Environ.*
457 *Toxicol. Chem.* **2004**, *23* (1), 41-48.
- 458 (20) Williams, A. G. B.; Scherer, M. M. Kinetics of Cr(VI) reduction by carbonate green rust.
459 *Environ. Sci. Technol.* **2001**, *35* (17), 3488-3494.
- 460 (21) O'Loughlin, E. J.; Kelly, S. D.; Kemner, K. M.; Csencsits, R.; Cook, R. E. Reduction of
461 Ag(I), Au(III), Cu(II), and Hg(II) by Fe(II)/Fe(III) hydroxysulfate green rust. *Chemosphere*
462 **2003**, *53* (5), 437-446.
- 463 (22) Guerbois, D.; Ona-Nguema, G.; Morin, G.; Abdelmoula, M.; Laverman, A. M.; Mouchel, J.
464 M.; Barthelemy, K.; Maillot, F.; Brest, J. Nitrite reduction by biogenic hydroxycarbonate green
465 rusts: Evidence for hydroxy-nitrite green rust formation as an intermediate reaction product.
466 *Environ. Sci. Technol.* **2014**, *48* (8), 4505-4514.
- 467 (23) Etique, M.; Zegeye, A.; Gregoire, B.; Carteret, C.; Ruby, C. Nitrate reduction by mixed
468 iron(II-III) hydroxycarbonate green rust in the presence of phosphate anions: The key parameters
469 influencing the ammonium selectivity. *Water Res.* **2014**, *62*, 29-39.
- 470 (24) Trolard, F. Fougerite: From field experiment to the homologation of the mineral. *C. R.*
471 *Geosci.* **2006**, *338* (16), 1158-1166.
- 472 (25) Berthelin, J.; Ona-Nguema, G.; Stemmler, S.; Quantin, C.; Abdelmoula, M.; Jorand, F.
473 Bioreduction of ferric species and biogenesis of green rusts in soils. *C. R. Geosci.* **2006**, *338* (6-
474 7), 447-455.
- 475 (26) Chaudhuri, S. K.; Lack, J. G.; Coates, J. D. Biogenic magnetite formation through anaerobic
476 biooxidation of Fe(II). *Appl. Environ. Microbiol.* **2001**, *67* (6), 2844-2848.
- 477 (27) Pantke, C.; Obst, M.; Benzerara, K.; Morin, G.; Ona-Nguema, G.; Dippon, U.; Kappler, A.
478 Green rust formation during Fe(II) oxidation by the nitrate-reducing *Acidovorax sp.* Strain
479 BoFeN1. *Environ. Sci. Technol.* **2012**, *46* (3), 1439-1446.
- 480 (28) Usman, M.; Hanna, K.; Abdelmoula, M.; Zegeye, A.; Faure, P.; Ruby, C. Formation of
481 green rust via mineralogical transformation of ferric oxides (ferrihydrite, goethite and hematite).
482 *Applied Clay Science* **2012**, *64*, 38-43.
- 483 (29) Etique, M.; Jorand, F. P. A.; Zegeye, A.; Gregoire, B.; Despas, C.; Ruby, C. Abiotic process
484 for Fe(II) oxidation and green rust mineralization driven by a heterotrophic nitrate reducing
485 bacteria (*Klebsiella mobilis*). *Environ. Sci. Technol.* **2014**, *48* (7), 3742-3751.
- 486 (30) O'Loughlin, E. J.; Gorski, C. A.; Scherer, M. M. Effects of phosphate on secondary mineral
487 formation during the bioreduction of akaganeite (β -FeOOH): Green rust versus framboidal
488 magnetite. *Curr. Inorg. Chem.* **2015**, *5* (3), 214-224.

- 489 (31) Etique, M.; Jorand, F. P. A.; Ruby, C. Magnetite as a precursor for green rust through the
490 hydrogenotrophic activity of the iron-reducing bacteria *Shewanella putrefaciens*. *Geobiology*
491 **2016**, *14* (3), 237-254.
- 492 (32) Zegeye, A.; Etique, M.; Carteret, C.; Ruby, C.; Schaaf, P.; Francius, G. Origin of the
493 differential nanoscale reactivity of biologically and chemically formed green rust crystals
494 investigated by chemical force spectroscopy. *J. Phys. Chem. C* **2014**, *118* (11), 5978-5987.
- 495 (33) Remy, P. P.; Etique, M.; Hazotte, A. A.; Sergent, A. S.; Estrade, N.; Cloquet, C.; Hanna, K.;
496 Jorand, F. P. A. Pseudo-first-order reaction of chemically and biologically formed green rusts
497 with Hg^{II} and C₁₅H₁₅N₃O₂: Effects of pH and stabilizing agents (phosphate, silicate, polyacrylic
498 acid, and bacterial cells). *Water Res.* **2015**, *70*, 266-278.
- 499 (34) O'Loughlin, E. J.; Kelly, S. D.; Cook, R. E.; Csencsits, R.; Kemner, K. M. Reduction of
500 uranium (VI) by mixed iron (II)/iron (III) hydroxide (green rust): Formation of UO₂
501 nanoparticles. *Environ. Sci. Technol.* **2003**, *37* (4), 721-727.
- 502 (35) O'Loughlin, E. J.; Kelly, S. D.; Kemner, K. M. XAFS investigation of the interactions of
503 U(VI) with secondary mineralization products from the bioreduction of Fe(III) oxides. *Environ.*
504 *Sci. Technol.* **2010**, *44* (5), 1656-1661.
- 505 (36) Latta, D. E.; Boyanov, M. I.; Kemner, K. M.; O'Loughlin, E. J.; Scherer, M. Reaction of
506 uranium(VI) with green rusts: Effect of interlayer anion. *Curr. Inorg. Chem.* **2015**, *5* (3), 156-
507 168.
- 508 (37) Brooks, S. C.; Fredrickson, J. K.; Carroll, S. L.; Kennedy, D. W.; Zachara, J. M.; Plymale,
509 A. E.; Kelly, S. D.; Kemner, K. M.; Fendorf, S. Inhibition of bacterial U(VI) reduction by
510 calcium. *Environ. Sci. Technol.* **2003**, *37* (9), 1850-1858.
- 511 (38) Génin, J. M. R.; Christy, A.; Kuzmann, E.; Mills, S.; Ruby, C. Structure and occurrences of
512 << green rust >> related new minerals of the fougérite group, trébeurdenite and mössbauerite,
513 belonging to the hydrotalcite supergroup; how Mössbauer spectroscopy helps XRD. *Hyperfine*
514 *Interact.* **2014**, *226* (1-3), 459-482.
- 515 (39) Refait, P.; Drissi, S. H.; Pytkiewicz, J.; Genin, J. M. R. The anionic species competition in
516 iron aqueous corrosion: Role of various green rust compounds. *Corrosion Science* **1997**, *39* (9),
517 1699-1710.
- 518 (40) Refait, P. H.; Abdelmoula, M.; Genin, J. M. R. Mechanisms of formation and structure of
519 green rust one in aqueous corrosion of iron in the presence of chloride ions. *Corrosion Science*
520 **1998**, *40* (9), 1547-1560.
- 521 (41) Lee, J. H.; Fredrickson, J. K.; Kukkadapu, R. K.; Boyanov, M. I.; Kemner, K. M.; Lin, X. J.;
522 Kennedy, D. W.; Bjornstad, B. N.; Konopka, A. E.; Moore, D. A.; Resch, C. T.; Phillips, J. L.
523 Microbial reductive transformation of phyllosilicate Fe(III) and U(VI) in fluvial subsurface
524 sediments. *Environ. Sci. Technol.* **2012**, *46* (7), 3721-3730.
- 525 (42) Stookey, L. L. Ferrozine---a new spectrophotometric reagent for iron. *Anal. Chem.* **1970**, *42*
526 (7), 779-781.
- 527 (43) Sowder, A. G.; Clark, S. B.; Fjeld, R. A. The effect of sample matrix quenching on the
528 measurement of trace uranium concentrations in aqueous solutions using kinetic phosphorimetry.
529 *J. Radioanal. Nucl. Chem.* **1998**, *234* (1-2), 257-260.
- 530 (44) Dong, W.; Brooks, S. C. Determination of the formation constants of ternary complexes of
531 uranyl and carbonate with alkaline earth metals (Mg²⁺, Ca²⁺, Sr²⁺, and Ba²⁺) using anion
532 exchange method. *Environ. Sci. Technol.* **2006**, *40* (15), 4689-4695.
- 533 (45) Ravel, B.; Newville, M. ATHENA, ARTEMIS, HEPHAESTUS: data analysis for X-ray
534 absorption spectroscopy using IFEFFIT. *J. Synchrotron Radiat.* **2005**, *12*, 537-541.

- 535 (46) Veeramani, H.; Scheinost, A. C.; Monsegue, N.; Qafoku, N. P.; Kukkadapu, R.; Newville,
536 M.; Lanzirrotti, A.; Pruden, A.; Murayama, M.; Hochella, M. F. Abiotic reductive immobilization
537 of U(VI) by biogenic mackinawite. *Environ. Sci. Technol.* **2013**, *47* (5), 2361-2369.
- 538 (47) Veeramani, H.; Alessi, D. S.; Suvorova, E. I.; Lezama-Pacheco, J. S.; Stubbs, J. E.; Sharp, J.
539 O.; Dippon, U.; Kappler, A.; Bargar, J. R.; Bernier-Latmani, R. Products of abiotic U(VI)
540 reduction by biogenic magnetite and vivianite. *Geochim. Cosmochim. Acta* **2011**, *75* (9), 2512-
541 2528.
- 542 (48) Dodge, C. J.; Francis, A. J.; Gillow, J. B.; Halada, G. P.; Eng, C.; Clayton, C. R.
543 Association of uranium with iron oxides typically formed on corroding steel surfaces. *Environ.*
544 *Sci. Technol.* **2002**, *36* (16), 3504-3511.
- 545 (49) Gu, B.; Liang, L.; Dickey, M. J.; Yin, X.; Dai, S. Reductive precipitation of uranium (VI) by
546 zero-valent iron. *Environ. Sci. Technol.* **1998**, *32* (21), 3366-3373.
- 547 (50) Yan, S.; Hua, B.; Bao, Z. Y.; Yang, J.; Liu, C. X.; Deng, B. L. Uranium(VI) removal by
548 nanoscale zerovalent iron in anoxic batch systems. *Environ. Sci. Technol.* **2010**, *44* (20), 7783-
549 7789.
- 550 (51) Alessi, D. S.; Uster, B.; Veeramani, H.; Suvorova, E. I.; Lezama-Pacheco, J. S.; Stubbs, J.
551 E.; Bargar, J. R.; Bernier-Latmani, R. Quantitative separation of monomeric U(IV) from UO₂ in
552 products of U(VI) reduction. *Environ. Sci. Technol.* **2012**, *46* (11), 6150-6157.
- 553 (52) Latta, D. E.; Mishra, B.; Cook, R. E.; Kemner, K. M.; Boyanov, M. I. Stable U(IV)
554 complexes form at high-affinity mineral surface sites. *Environ. Sci. Technol.* **2014**, *48* (3), 1683-
555 1691.
- 556 (53) Fletcher, K. E.; Boyanov, M. I.; Thomas, S. H.; Wu, Q. Z.; Kemner, K. M.; Löffler, F. E.
557 U(VI) reduction to mononuclear U(IV) by *Desulfitobacterium* species. *Environ. Sci. Technol.*
558 **2010**, *44* (12), 4705-4709.
- 559 (54) Dusausoy, Y.; Ghermani, N. E.; Podor, R.; Cuney, M. Low-temperature ordered phase of
560 CaU(PO₄)₂: Synthesis and crystal structure. *Eur. J. Mineral.* **1996**, *8* (4), 667-673.
- 561 (55) Boyanov, M. I.; O'Loughlin, E. J.; Roden, E. E.; Fein, J. B.; Kemner, K. M. Adsorption of
562 Fe(II) and U(VI) to carboxyl-functionalized microspheres: The influence of speciation on uranyl
563 reduction studied by titration and XAFS. *Geochim. Cosmochim. Acta* **2007**, *71* (8), 1898-1912.
- 564 (56) Bone, S. E.; Dynes, J. J.; Cliff, J.; Bargar, J. R. Uranium(IV) adsorption by natural organic
565 matter in anoxic sediments. *Proc. Natl. Acad. Sci. U. S. A.* **2017**, *114* (4), 711-716.
- 566 (57) Furukawa, Y.; Kim, J. W.; Watkins, J.; Wilkin, R. T. Formation of ferrihydrite and
567 associated iron corrosion products in permeable reactive barriers of zero-valent iron. *Environ.*
568 *Sci. Technol.* **2002**, *36* (24), 5469-5475.
- 569 (58) Phillips, D. H.; Watson, D. B.; Roh, Y.; Gu, B. Mineralogical characteristics and
570 transformations during long-term operation of a zerovalent iron reactive barrier. *J. Environ.*
571 *Qual.* **2003**, *32* (6), 2033-2045.
- 572 (59) McCormick, M. L.; Kim, H. S.; Bouwer, E. J.; Adriaens, P. *Abiotic transformation of*
573 *chlorinated solvents as a consequence of microbial iron reduction: An investigation of the role of*
574 *biogenic magnetite in mediating reductive dechlorination*, In: Proceedings of the Thirtieth Mid-
575 Atlantic Industrial and Hazardous Waste Conference-Hazardous and Industrial Wastes.
576 Technomic Publishing Company, Inc., pp 339-348.
- 577 (60) Stewart, B. D.; Neiss, J.; Fendorf, S. Quantifying constraints imposed by calcium and iron
578 on bacterial reduction of uranium(VI). *J. Environ. Qual.* **2007**, *36* (2), 363-372.
- 579
580

581
582



For table of contents only

583
584
585
586